Peroxynitrite-Mediated Decarboxylation of Pyruvate to Both Carbon Dioxide and Carbon Dioxide Radical Anion

ARTICLE *in* CHEMICAL RESEARCH IN TOXICOLOGY · AUGUST 1997

Impact Factor: 3.53 · DOI: 10.1021/tx970031g · Source: PubMed

4 AUTHORS, INCLUDING:

Ana Denicola
University of the Republic, Uruguay
86 PUBLICATIONS **3,834** CITATIONS
SEE PROFILE

Rafael Radi
University of the Republic, Uruguay
310 PUBLICATIONS **22,609** CITATIONS
SEE PROFILE

Ohara Augusto
University of São Paulo
159 PUBLICATIONS **5,004** CITATIONS
SEE PROFILE

Peroxynitrite-Mediated Decarboxylation of Pyruvate to Both Carbon Dioxide and Carbon Dioxide Radical Anion

Jeannette Vásquez-Vivar, Ana Denicola,† Rafael Radi,† and Ohara Augusto*

Departamento de Bioquímica, Instituto de Química, Universidade de São Paulo, CxP 26077, 05599-970 São Paulo, SP, Brazil, and Department of Biochemistry, Facultad de Medicina, Universidad de la República, 11800 Montevideo, Uruguay

Received February 25, 1997[⊗]

There has been a recent renewal of interest in the antioxidant properties of pyruvate which are usually attributed to its capacity to undergo oxidative decarboxylation in the presence of hydrogen peroxide. The interaction of pyruvate with other oxidizing biological intermediates, however, has been scarcely considered in the literature. Here we report that peroxynitrite, the oxidant produced by the reaction between superoxide anion and nitric oxide, reacts with pyruvate with an apparent second-order rate constant of 88 ± 7 M^{-1} s^{-1} at pH 7.4 and 37 °C. Kinetic studies indicated that pyruvate reacts with peroxynitrite anion (k = 100 ± 7 M^{-1} s^{-1}), peroxynitrous acid (k = 49 ± 7 M^{-1} s^{-1}), and a highly oxidizing species derived from peroxynitrous acid. Pyruvate decarboxylation was proved by anion exchange chromatography detection of acetate in incubations of peroxynitrite and pyruvate at pH 7.4 and 5.5. Formation of carbon dioxide radical anion was ascertained by EPR spin-trapping studies in the presence of GSH and the spin-trap 5,5-dimethyl-1-pyrroline *N*-oxide (DMPO). The use of pyruvate labeled with ^{13}C at the 1-position led to the detection of the labeled DMPO carbon dioxide radical anion adduct. In the absence of GSH, oxygen consumption studies confirmed that peroxynitrite mediates the decarboxylation of pyruvate to free radical intermediates. Comparing the yields of acetate and free radicals estimated from the oxygen uptake studies, it is concluded that pyruvate is oxidized by both one- and two-electron oxidation pathways, the latter being preponderant. Hydrogen peroxide-mediated pyruvate oxidation does not produce detectable levels of carbon dioxide radical anion except in the presence of iron(II)−ethylenediamine-*N*,*N*,*N*′,*N*′-tetraacetate (EDTA). The apparent second-order rate constant of the reaction between pyruvate and hydrogen peroxide was determined to be 1 order of magnitude lower than that of the reaction between pyruvate and peroxynitrite. The latter process may contribute to the antioxidant properties of pyruvate.

Introduction

Pyruvate is an ubiquitous cellular metabolite which affects a variety of physiological and biochemical functions. When consumed or infused at supraphysiologic concentrations in man and animals, pyruvate can induce a multitude of beneficial metabolic effects ranging from normalization of plasma hypoglycemia in non-insulin-dependent diabetes (*1*) to inhibition of malignant growth (*2*). Although it is doubtful that pyruvate induces this myriad of responses through only one mechanism, there has been renewed interest in the antioxidant properties of pyruvate as a possible mechanism underlying some of its physiological effects (*3*). Recently, pyruvate has been shown to protect against oxidative damage promoted by various insults such as denaturation of lens proteins induced by xanthine/xanthine oxidase (*4*), myocardial injury after ischemia-reperfusion (*5, 6*), renal injury mediated by hydrogen peroxide (*7*), and peroxisomal proliferation induced by clofibrate (*8*).

The antioxidant properties of pyruvate and other α-keto acids are considered to be primarily dependent on their capacity of undergoing nonenzymatic decarboxylation in the presence of hydrogen peroxide, a reaction first described in 1904 (*9*). Through this reaction, the α-keto acid is converted to a carboxylic acid, and carbon dioxide is produced while hydrogen peroxide is detoxified to water (eq 1):

$$CH_3COCOO^- + H_2O_2 \rightarrow CH_3COO^- + CO_2 + H_2O \quad (1)$$

Reactions between pyruvate and oxidizing biological intermediates other than hydrogen peroxide, however, have been scarcely considered in the literature. One oxidant of emerging biological importance is peroxynitrite[1] which is formed by the fast combination reaction (k = 4−7 × 10^9 M^{-1} s^{-1}) (*10, 11*) between nitrogen monoxide and superoxide radical anion (eq 2):

$$O_2^{\bullet -} + {}^{\bullet}NO \rightarrow ONOO^- \quad (2)$$

Since peroxynitrite is a stronger oxidant than both nitric oxide and superoxide anion, it has been suggested to be the oxidant responsible for some of the pathological conditions associated with an overproduction of these radicals (*12*). Indeed, peroxynitrite appears to be formed *in vivo* (*13*−*15*) and is a versatile oxidant that reacts with

* Address correspondence to this author. Telephone: 55-11-818-3873. Fax: 55-11-8187986 and 55-11-815-5579. E-mail: oaugusto@quim.iq.usp.br.

† Universidad de la República.

⊗ Abstract published in *Advance ACS Abstracts,* June 1, 1997.

[1] The term peroxynitrite is used to refer to the sum of all possible conformers of peroxynitrite anion ($ONOO^-$) and peroxynitrous acid (ONOOH) unless otherwise specified. IUPAC-recommended names for peroxynitrite anion, peroxynitrous acid, and nitric oxide are oxoperoxynitrate(−1), hydrogen oxyperoxynitrate, and nitrogen monoxide, respectively.

S0893-228x(97)00031-3 CCC: $14.00

most biomolecules by mechanisms which remain under active investigation (*16*−*18*).

The peroxynitrite anion is stable at alkaline solution, but its acid rearranges to nitrate in a first-order kinetic process (eqs 3, 4). Kinetic studies indicate that molecules which are present during peroxynitrite decomposition can be oxidized either by reacting directly with peroxynitrite or after the acid rearranges to a highly oxidizing species which may be a vibrationally activated state of peroxynitrous acid (ONOOH*) ($E^o = 2.1$ V) (*16*) whose reactivity is close to that of the hydroxyl radical (*16*−*18*). Moreover, substrate oxidation can occur by both one- and two-electron transfer processes (*19*−*22*). *In vivo*, other oxidative reactions are also possible because peroxynitrite anion reacts rapidly with carbon dioxide, one of the most abundant constituents of the extracelluar milieu, forming an adduct which displays oxidizing properties (*23*−*26*).

$$ONOO^- + H^+ \underset{pK_a = 6.8}{\rightleftharpoons} ONOOH \qquad (3)$$

$$ONOOH \rightarrow NO_3^- + H^+ \qquad (4)$$

The possible role of peroxynitrite as a key intermediate in oxidative damage, its higher reactivity as compared with hydrogen peroxide, and the renewed interest in the antioxidant properties of α-keto acids led us to examine the reaction between pyruvate and peroxynitrite. Our results demonstrate that peroxynitrite promotes the oxidative decarboxylation of pyruvate to acetate but, distinct from hydrogen peroxide, it also produces the carbon dioxide radical anion. Peroxynitrite-mediated decarboxylation of amino acids and other organic acids has been previously proposed to explain the data obtained from the Viking Lander Missons testing for life signs on Mars (*27*).

Experimental Procedures

Chemicals. GSH, 5,5-dimethyl-1-pyrroline *N*-oxide (DMPO),[2] Chelex-100, diethylenetriamine-*N*,*N*,*N*′,*N*″-pentaacetate (DTPA), and manganese dioxide were obtained from Sigma Chemical Co. (St. Louis, MO). Sodium pyruvate-*1*-^{13}C was obtained from Isotec Inc. (Miamisburg, OH). Sodium pyruvate, sodium acetate, sodium nitrite, sodium azide, iron sulfate, and ethylenediamine-*N*,*N*,*N*′,*N*′-tetraacetate (EDTA) were obtained from Merck (Darmstadt, Germany). Hydrogen peroxide was obtained from Fisher Scientific (Pittsburgh, PA). DMPO was purified by vacuum distillation (*28*). Peroxynitrite was synthesized either by reaction between hydrogen peroxide and sodium nitrite in a quenched flow reactor (*29*) or by ozonation of azide solutions (*30*) and was kept frozen at −80 °C. Stock solutions of peroxynitrite obtained by the first method were maintained on manganese dioxide throughout use to eliminate any hydrogen peroxide contamination. The concentration of peroxynitrite was determined spectrophotometrically at 302 nm using an extinction coefficient of 1670 M^{-1} cm^{-1} (*29*). When required, peroxynitrite working solutions were diluted in 0.1 N NaOH. All solutions were prepared in distilled water treated in a Millipore Milli-Q system.

Kinetic Studies. The rate of peroxynitrite decomposition in the absence and presence of pyruvate was monitored at 302 nm in a stopped flow spectrophotometer (Applied Photophysics SF.17MV) with a mixing time of less than 2 ms. Apparent rate constants for the reaction of pyruvate with peroxynitrite, k_{obs} (s^{-1}), were determined by nonlinear least-squares fitting of stopped flow data to a single-exponential function with a nonzero offset. Reported values are the average ± standard deviation of at least seven separate determinations. The temperature was maintained constant at 37 ± 0.2 °C, and the pH of the reaction mixtures was determined at the outlet.

The disappearance of hydrogen peroxide (1 mM) in the presence of pyruvate (10 mM) in 0.1 M phosphate buffer, pH 7.4 and 5.8, at 37 °C was monitored by taking aliquots of the incubation mixtures at different times and determining the remaining hydrogen peroxide through the oxidation of 2,2′-azinobis(3-ethylbenzothiazoline sulfonate) (ABTS) catalyzed by horseradish peroxidase as previously described (*31*).

Data fitting was performed using Origin 3.73 (Microcal Software, Inc.), and graphics were generated in Slide Write Plus (Advanced Graphics Software).

EPR Spin-Trapping Experiments. EPR spectra were recorded at room temperature using a Bruker ER 200 D-SRC spectrometer. In the experiments with peroxynitrite, all spectra were recorded 1 min after the addition of the oxidant and the pH was measured at the end of the experiment to detect changes caused by the addition of alkaline stock solutions of peroxynitrite.

Oxygen Consumption. Oxygen uptake studies were performed using an oxygen monitor (Gilson 5/6 oxygraph at 30 °C). The saturating oxygen concentration at this temperature was taken to be 220 μM (*32*).

Anion Exchange Chromatography. Acetate analysis was performed using a Dionex chromatograph equipped with a conductivity detector. Reaction mixtures were prepared in water and their pHs controlled by the addition of HCl and/or NaOH. In the case of peroxynitrite-mediated oxidations, aliquots of HCl and of peroxynitrite stock solutions were pipetted onto different sites of the reaction tube wall and mixed together with the other reagents in order to achieve the desired final pH which was always checked. Peroxynitrite- and hydrogen peroxide-mediated oxidations were stopped by 400 dilution with water after 5 and 30 min of incubation, respectively. The diluted samples were injected onto an Ion-Pac AS5A column (5 μm) and eluted with 0.1 mM NaOH at flow rates of 1 mL/min. Under these conditions acetate and pyruvate separated well with elution times of 2.6 and 4.1 min, respectively. Authentic acetate was used as standard for quantification.

Results

Kinetic Studies. A direct reaction between pyruvate and peroxynitrite was demonstrated by the acceleration of peroxynitrite decomposition at 302 nm in the presence of pyruvate. Peroxynitrite decay followed pseudo-first-order kinetics, and plots of the pseudo-first-order rate constant (k_{obs}) as a function of pyruvate concentration gave an apparent bimolecular rate constant in the range of 80 M^{-1} s^{-1} at pH 7.4 and 37 °C (Figure 1). However, the plot intercept from a linear regression using pyruvate concentrations above 1 mM would result in a k_{obs} value for the decomposition of peroxynitrite in the absence of substrate higher than the value measured, 0.80 ± 0.04 s^{-1} (Figure 1, inset), which is in agreement with previously reported values (*19*, *33*). This kinetic behavior in which a downward curvature is observed at low substrate concentrations with linear fitting at higher concentrations has been observed before for peroxynitrite-mediated oxidation of methionine (*19*), ascorbate (*34*), and tryptophan (*35*). These results were interpreted as an indication that the substrate reacts with both ground and activated (ONOOH*) forms of peroxynitrite (*19*, *34*, *35*). Consequently, pyruvate would also react with both forms of peroxynitrite, and therefore the calculation of the apparent second-order rate constants requires a more

[2] Abbreviations: ABTS, 2,2′-azinobis(3-ethylbenzothiazoline sulfonate); DMPO, 5,5-dimethyl-1-pyrroline *N*-oxide; DTPA, diethylenetriamine-*N*,*N*,*N*′,*N*″-pentaacetate; EDTA, ethylenediamine-*N*,*N*,*N*′,*N*′-tetraacetate; PBN, *N*-*tert*-butyl-α-phenylnitrone; POBN, α-(4-pyridyl 1-oxide)-*N*-*tert*-butylnitrone; Pyr, pyruvate.

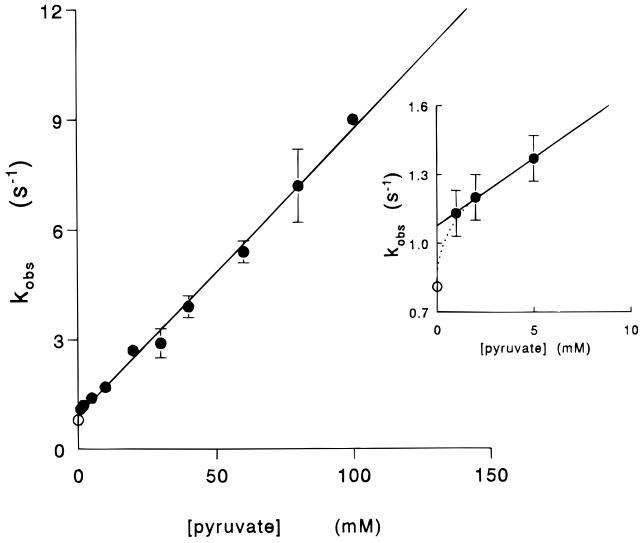

Figure 1. Pseudo-first-order rate constants for the reaction between peroxynitrite and pyruvate as a function of pyruvate concentration. The initial peroxynitrite concentration was 250 μM, and reactions were performed in 0.1 M phosphate buffer (pH 7.44) containing 0.1 mM DTPA, 37 °C. The straight line was obtained by linear regression fitting of the experimental data. The inset shows the dependency of the pseudo-first-order rate constants as a function of low pyruvate concentrations (0−5 mM).

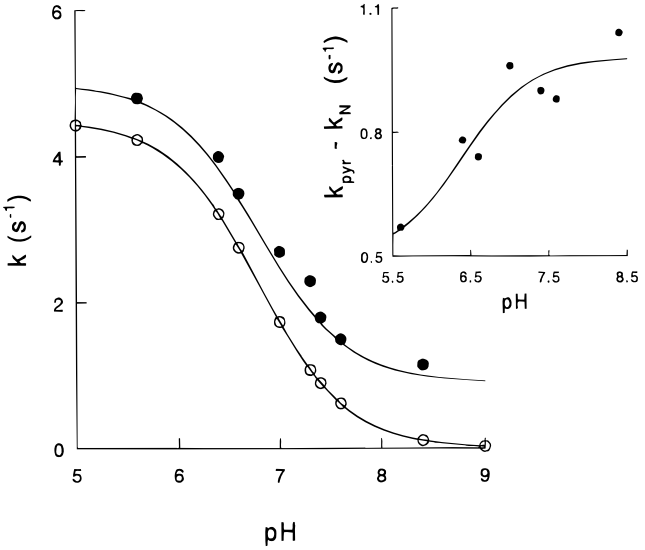

Figure 2. Rates of peroxynitrite (250 μM) decomposition in 0.1 M phosphate buffer containing 0.1 mM DTPA measured in the absence (○), k_N, and presence (●), k_{pyr}, of 10 mM pyruvate and plotted as a function of final pH. The inset shows the dependence with pH of the difference of incubating with 10 mM pyruvate in 0.1 M phosphate buffer containing 0.1 mM DTPA at 37 °C ($k_{pyr} - k_N$).

detailed kinetic analysis (see below, eqs 11 and 12) than obtaining them from the slope of Figure 1.

The pH profile (Figure 2) indicates that there is more than one reactivity between the ground state forms of peroxynitrite and pyruvate. The pH dependency in the presence of pyruvate results on a single apparent pK_a of 6.9, which is in good agreement with that determined for peroxynitrous acid (*17*, *35*). The dissociation of pyruvate would not be involved in the pH range studied as its pK_a is 2.3. However, at alkaline pHs, the k_{obs} values have an offset that remains considerably higher (Figure 2) than those expected for reactions depending only on peroxynitrous acid, suggesting that peroxynitrite anion also participates in the process (*35*). Moreover, the difference of k_{obs} in the presence and absence of pyruvate (Figure 2, inset) strongly suggests that the reaction of peroxynitrite anion is faster than that of the acid. Thus kinetic analysis was formulated assuming that pyruvate reacts with peroxynitrite anion, ground state peroxynitrous acid, and activated peroxynitrous acid with the latter being formed in a steady state (eqs 5−10).

$$\mathrm{ONOOH} \overset{K_a}{\rightleftharpoons} \mathrm{ONOO^-} + \mathrm{H^+} \quad (5)$$

$$\mathrm{ONOOH} \underset{k_{-1}}{\overset{k_1}{\rightleftharpoons}} \mathrm{ONOOH^*} \quad (6)$$

$$\mathrm{ONOOH^*} \xrightarrow{k_N} \mathrm{NO_3^-} + \mathrm{H^+} \quad (7)$$

$$\mathrm{ONOO^-} + \mathrm{Pyr} \xrightarrow{k_C} \mathrm{products} \quad (8)$$

$$\mathrm{ONOOH} + \mathrm{Pyr} \xrightarrow{k_S} \mathrm{products} \quad (9)$$

$$\mathrm{ONOOH^*} + \mathrm{Pyr} \xrightarrow{k_0} \mathrm{products} \quad (10)$$

According to these reactions, k_{obs} is given by eq 11:

$$k_{obs} = \left(\frac{k_S[H^+] + K_a k_C}{k_A + [H^+]}\right)[Pyr] + \left(\frac{k_1 k_0 [Pyr] + k_N k_1}{k_N + k_{-1} + k_0[Pyr]}\right)\left(\frac{[H^+]}{K_a + [H^+]}\right) \quad (11)$$

At relatively high pyruvate concentrations, in which its reaction with the energized intermediate (ONOOH*) competes well with isomerization (i.e., $k_0[Pyr] \gg k_N$), k_{obs} for the oxidation of pyruvate would be given by eq 12:

$$k_{obs} = \left(\frac{k_S[H^+] + K_a k_C}{K_a + [H^+]}\right)[Pyr] + k_1\left(\frac{[H^+]}{K_a + [H^+]}\right) \quad (12)$$

Thus, substituting in eq 12 the known values of K_a (1.59×10^{-7} M^{-1}), k_1 (4.5 s^{-1} at 37 °C) (*16*−*18*), and the pyruvate concentration (10 mM), the values of k_S and k_C were obtained by fitting data of Figure 2 (k_{obs} as a function of pH). The second-order rate constants estimated for k_S and k_C were 49 ± 9 and 100 ± 7 M^{-1} s^{-1}, respectively, resulting in an apparent second-order rate constant of 88 ± 7 M^{-1} s^{-1} at pH 7.4 and 37 °C, which is close to the experimental value obtained from the slope of Figure 1. Similar rate constant values were obtained when using data at higher pyruvate concentrations (i.e., 20 mM; data not shown). Therefore, the reaction of pyruvate with peroxynitrite anion is faster than the reaction with ground state peroxynitrous acid.

Overall, the apparent bimolecular rate constant of the reaction between pyruvate and peroxynitrite at pH 7.4, 37 °C, is not high (88 ± 7 M^{-1} s^{-1}) but is higher than that expected for the reaction of pyruvate with hydrogen peroxide. The intermolecular rate constant of the latter reaction catalyzed by the hydroxyl anion at 20.7 °C and ionic strength of 1.0 has been reported to be 6.8×10^9 M^{-2} min^{-1} (*36*), given an estimated value of 28.5 M^{-1} s^{-1} for the apparent second-order rate constant at pH 7.4. Since the latter is influenced by general buffer and transition metal ion catalysis (*36*), we redetermined the second-order rate constant under our experimental con-

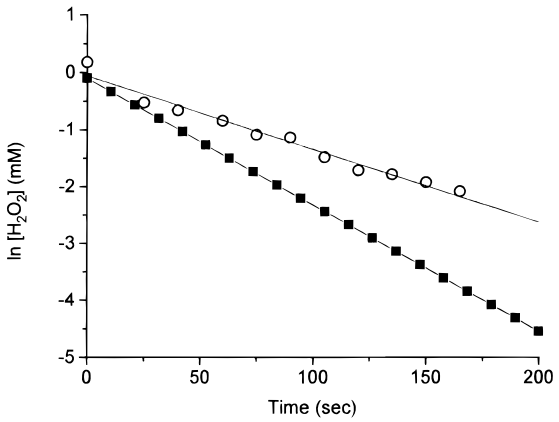

Figure 3. Plot of ln of hydrogen peroxide concentrations versus time in incubations containing excess pyruvate. Peroxynitrite (10 mM) was incubated with 1 mM hydrogen peroxide, 0.1 M phosphate buffer containing 0.1 mM DTPA at 37 °C at pH 5.8 (○) and 7.4 (□).

ditions, i.e., 0.1 M phosphate buffer containing 0.1 mM DTPA at 37 °C for comparative purposes. The obtained values were 1.2 and 2.2 M^{-1} s^{-1} at pH 5.8 and 7.4, respectively (Figure 3).

Formation of Carbon Dioxide Radical Anion. Formation of carbon dioxide radical anion during peroxynitrite-mediated oxidation of pyruvate was ascertained by EPR spin-trapping and oxygen consumption experiments.

Incubations of pyruvate with peroxynitrite in the presence of the spin-traps DMPO, *N-tert*-butyl-α-phenylnitrone (PBN), or α-(4-pyridyl 1-oxide)-*N-tert*-butylnitrone (POBN) led to the detection of very low levels of EPR signals as reported before in other peroxynitrite-mediated oxidations due to the fast decay of free radical adducts in the presence of this oxidant (*20*, *28*). In the presence of thiols which protect the adducts from decay (*20*, *28*), however, pyruvate-derived free radical adducts were easily detectable. For instance, incubation of pyruvate (30 mM) with peroxynitrite (0.5 mM) in the presence of DMPO (100 mM) and GSH (0.5 mM) in 0.1 M phosphate buffer (pH 7.4) containing 0.1 mM DTPA led to the detection of the EPR spectrum shown in Figure 4A. This spectrum is a composite of the EPR spectrum of two different radical adducts: the DMPO-hydroxyl radical (a^N = 1.49 mT, a^H = 1.49 mT) and a carbon-centered radical (a^N = 1.59 mT, a^H = 1.89 mT). The DMPO-hydroxyl radical adduct is formed by oxidation of the spin-trap by peroxynitrite (*20*, *37*, *38*), whereas the carbon-centered radical adduct should be derived from pyruvate, and indeed, it has hyperfine splitting constants consistent with the DMPO-carbon dioxide radical anion adduct (*39*) (Figure 4A). The identity of the latter species was confirmed by incubation of peroxynitrite with [^{13}C]-pyruvate labeled at the carboxyl group (Figure 4B,C). In this case, the six-line EPR spectrum of the DMPO-carbon dioxide radical anion adduct (Figure 4A) was substituted by an eleven-line EPR spectrum (a^N = 1.59 mT, a^H = 1.89 mT, a^{13C} = 1.23 mT) due to the contribution of ^{13}C atom (I = 1/2) (Figure 4B, C) (*39*). Similar results were obtained in the presence of the spin-trap PBN which rendered the corresponding PBN-carbon dioxide radical anion adducts: a six-line (a^N = 1.59 mT, a^H = 0.46 mT) and a twelve-line (a^N = 1.59, a^H = 0.46, a^{13C} = 1.18 mT) EPR spectrum (*40*) for unlabeled and labeled pyruvate, respectively (not shown).

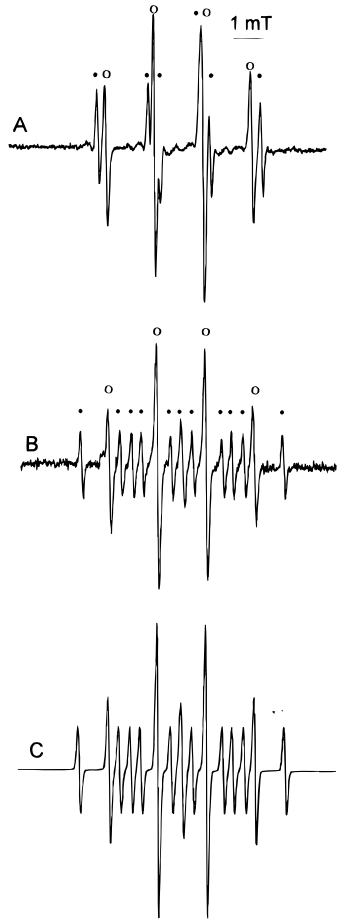

Figure 4. EPR spectra of DMPO radical adducts obtained during peroxynitrite decomposition in the presence of pyruvate and GSH. The spectra were obtained after 1 min of incubation at room temperature of 0.1 M DMPO, 0.5 mM GSH, and 0.5 mM peroxynitrite in 0.1 M phosphate buffer (pH 7.4) containing 0.1 mM DTPA in the presence of (A) 30 mM pyruvate and (B) 50 mM [1-^{13}*C*]pyruvate. (C) Computer simulation of panel B considering two radical adducts, DMPO-OH and DMPO-carbon dioxide radical anion, labeled with ^{13}C. The composite spectra of panels A and B were labeled to show their components: (○) DMPO-OH and (●) DMPO-CO_2^- and DMPO-$^{13}CO_2^-$ in panels A and B, respectively. Instrumental conditions: microwave power, 20 mW; modulation amplitude, 0.1 mT; time constant, 0.2 s; scan rate, 0.05 mT/s; gain, 1.25 × 10^5 (A) and 2.5 × 10^5 (B).

The yield of DMPO-carbon dioxide radical anion obtained during the oxidation of pyruvate by peroxynitrite (0.5 mM) in the presence of GSH (0.5 mM) increased with pyruvate concentrations leveling off at about 10 mM. EPR spin-trapping experiments with DMPO were also performed with peroxynitrite obtained by ozonation of azide solutions to completely exclude hydrogen peroxide contamination from peroxynitrite synthesis (*30*). In the latter case, yields of both the DMPO-carbon dioxide radical anion and DMPO-hydroxyl radical adducts comparable to those shown in Figure 4A were obtained, but trace amounts of the DMPO-azidyl radical adduct (a^N = 1.48 mT, a^H = 1.42 mT, $a^{N\beta}$ = 0.31 mT) (*41*) were also detected, indicating contamination of peroxynitrite by unreacted azide.

In contrast with the oxidation of pyruvate by peroxynitrite, no carbon dioxide radical anion could be detected during the process mediated by hydrogen peroxide. Incubations up to 30 min of high concentrations of hydrogen peroxide (50−300 mM) with pyruvate (50 mM) and DMPO (100 mM) in phosphate buffer (pH 7.4)

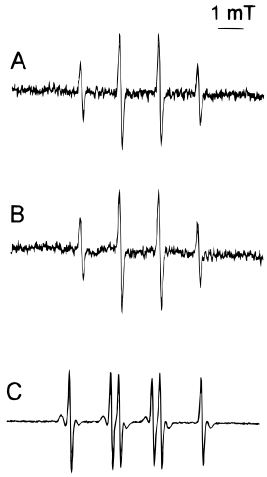

Figure 5. EPR spectra of DMPO radical adducts obtained during incubations of pyruvate with hydrogen peroxide in the absence and presence of iron(II)−EDTA. In the absence of iron(II)−EDTA, the spectra were obtained after 30 min of incubation at room temperature of 50 mM pyruvate with 100 mM DMPO in 0.1 M phosphate buffer (pH 7.4) containing 0.1 mM DTPA with (A) 50 mM hydrogen peroxide and (B) 100 mM hydrogen peroxide. Spectrum C was obtained after 1 min of incubation at room temperature of 50 mM pyruvate with 50 mM DMPO, 1.0 mM iron(II)−EDTA, and 2 mM hydrogen peroxide in phosphate buffer (pH 7.4). Instrumental conditions: microwave power, 20 mW; modulation amplitude, 0.1 mT; time constant, 0.2 s; scan rate, 0.05 mT/s; gain, 1.25×10^6 (A and B) and 1.25×10^5 (C).

containing 0.1 mM DTPA led only to the detection of trace amounts of the DMPO-hydroxyl radical adduct (Figure 5 A,B) which was probably produced from secondary reactions of the spin-trap (*42*). Although pyruvate oxidation by hydrogen peroxide alone did not produce pyruvate-derived free radicals (Figure 5A,B), low concentrations of hydrogen peroxide (2 mM) in the presence of iron(II)−EDTA (1.0 mM) produced the DMPO-carbon dioxide radical anion which was already detectable 1 min after the beginning of the reaction (Figure 5C). Under these conditions, the DMPO-hydroxyl radical adduct was barely detectable (Figure 5C) indicating that formation of the carbon dioxide radical was not dependent on the formation of the hydroxyl radical through the reaction between hydrogen peroxide and iron(II)−EDTA (*43*). In this case, the DMPO-hydroxyl radical would be detectable because the hydroxyl radical reacts faster with DMPO ($k = 3.4 \times 10^9$ M^{-1} s^{-1}) (*44*) than with pyruvate (3.1×10^7 M^{-1} s^{-1}) (*45*).

The ability of both peroxynitrite and hydrogen peroxide/iron(II)−EDTA to promote the oxidative decarboxylation of other α-keto acids to the carbon dioxide radical anion was tested with α-ketoglutaric acid. As shown in Figure 6, the DMPO-carbon dioxide radical adduct was detected in both systems although in a lower yield than obtained during pyruvate oxidation (Figures 4A, 5C). This suggests that α-ketoglutarate is less reactive than pyruvate toward both peroxynitrite and hydrogen peroxide/iron(II)−EDTA. In agreement, during the oxidation by the latter system it was also possible to detect the four-line spectrum of the DMPO-hydroxyl radical adduct (Figure 6B), indicating the occurrence of the Fenton reaction (*43*) in competition with the attack of hydrogen peroxide on the carbonyl group of the α-keto acid (see Scheme 1).

Carbon dioxide radical anion is a strong reducing species which reacts with oxygen with a rate constant of 2×10^9 M^{-1} s^{-1} (*46*), and its formation during peroxynitrite-mediated oxidation of pyruvate should result in oxygen consumption. Indeed, addition of peroxynitrite (1 mM) to pyruvate solutions (50 mM) led to fast oxygen consumption (Figure 7D), whereas peroxynitrite alone decomposed with oxygen evolution (Figure 7A) as previously described (*47*). The total oxygen consumed by 50 mM pyruvate and 1 mM peroxynitrite at pH 5.1 was 37 μM (Figure 7D) which corresponds to about 4% of the initial peroxynitrite concentration; at pH 7.4, the consumed oxygen corresponded to about 2% of the initial peroxynitrite concentration (Table 1).

It is important to note that oxygen consumption triggered by the peroxynitrite-mediated oxidation of pyruvate is not dependent on the presence of GSH (Figure 7D) further confirming that free radical formation results from the attack of pyruvate by peroxynitrite. Also, oxygen consumption is not followed by oxygen evolution (Figure 7D) as could be anticipated to result from the

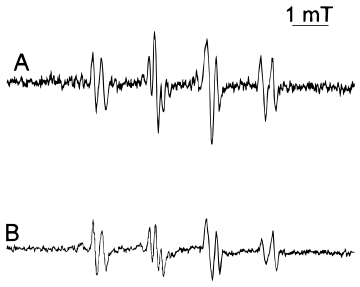

Figure 6. EPR spectra of DMPO radical adducts obtained during the oxidation of α-ketoglutaric acid by peroxynitrite and hydrogen peroxide/iron(II)−EDTA. The spectra were obtained after 1 min of incubation at room temperature of 50 mM α-ketoglutaric acid in the presence of 0.1 M DMPO in 0.1 M phosphate buffer (pH 7.4) containing 0.1 mM DTPA with (A) 0.5 mM peroxynitrite plus 0.5 mM GSH and (B) 2 mM hydrogen peroxide plus 1.0 mM iron(II)−EDTA. Instrumental conditions: microwave power, 20 mW; modulation amplitude, 0.1 mT; time constant, 0.2 s; scan rate, 0.05 mT/s; gain, 5×10^5 (A) and 2×10^5 (B).

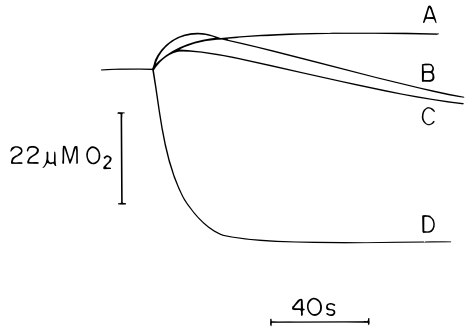

Figure 7. Oxygen consumption during peroxynitrite-mediated oxidation of pyruvate. Peroxynitrite (1 mM) was added to 0.1 M phosphate buffer (pH 5.1) containing 0.1 mM DTPA at 30 °C and (A) nothing, (B) 10 mM bicarbonate, (C) 50 mM pyruvate plus 10 mM bicarbonate, and (D) 50 mM pyruvate.

Scheme 1

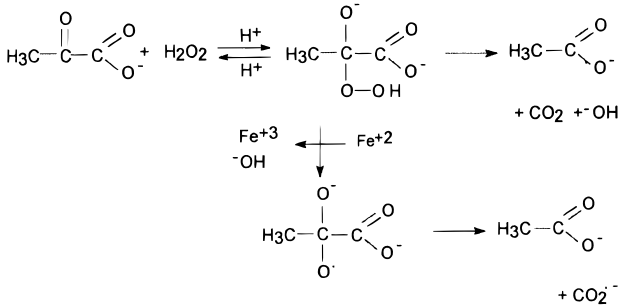

Table 1. Oxygen Consumption during Peroxynitrite-Mediated Oxidation of Pyruvate

system	pH changes in the incubation mixtures	oxygen uptake[a] (μM)
pyruvate (50 mM) + $ONOO^-$ (1.0 mM)	5.1	36.6 ± 4.3
	5.7	22.6 ± 2.0
	6.7	20.3 ± 2.2
	7.5	19.7 ± 2.5
	8.1	not detectable

[a] Oxygen uptake was measured in 0.1 M phosphate at 30 °C as described in the Experimental Procedures. The values were calculated without discounting the oxygen evolved during peroxynitrite decomposition in the absence of pyruvate (see, for instance, Figure 7) and correspond to the mean ± SD of three independent experiments.

dismutation of the superoxide anion produced by the reaction of the carbon dioxide radical anion with oxygen. Indeed, oxygen consumption followed by an oxygen evolution that can be inhibited by superoxide dismutase was observed during peroxynitrite-mediated oxidation of formate,[3] a process which also produces the carbon dioxide radical anion (*20*). This comparison indicates that during the peroxynitrite-mediated pyruvate decarboxylation, oxygen may also be consumed by free radicals other than carbon dioxide radical anion. The latter has been reported to react with pyruvate producing secondary free radicals (*48*) which could also consume oxygen. Under our experimental conditions, however, it was impossible to detect these secondary free radicals by spin-trapping experiments (Figures 4−6).

It is known that peroxynitrite reacts fast with carbon dioxide ($k = 3-5.9 \times 10^4$ M^{-1} s^{-1}) (*23*−*26*) which is produced during pyruvate decarboxylation, and consequently, we examined the effects of the carbon dioxide/bicarbonate pair on the oxygen consumption triggered by peroxynitrite. Bicarbonate (10 mM) inhibited oxygen consumption by pyruvate at pH 5.1 in a complex way (Figure 7C). In the initial stages, some oxygen evolution was observed, but then oxygen consumption started although at a much lower rate than that observed in the absence of bicarbonate (Figure 7C,D). This anion behaved similarly in the absence of pyruvate, marginally affecting the initial oxygen evolution observed during peroxynitrite decomposition but rapidly turning it into a slow oxygen consumption (Figure 7A,B). Although these results indicate multiple competitive reactions, they suggest that bicarbonate is able to inhibit peroxynitrite-mediated decarboxylation of pyruvate to the carbon dioxide radical anion. Accordingly, no DMPO-carbon dioxide radical anion adduct could be detected in incubations of pyruvate with peroxynitrite in the presence of 10 mM bicarbonate at pH 7.4, although the yield of the DMPO-hydroxyl radical adduct was increased (Figure 8B,D). At 1 mM concentration, bicarbonate inhibited the DMPO-carbon dioxide radical anion by 30% (Figure 8B,C). This concentration-dependent inhibition at pH 7.4 is in reasonable agreement with those expected from the apparent rate constants of peroxynitrite with pyruvate (88 M^{-1} s^{-1}) and bicarbonate (2.3×10^3 M^{-1} s^{-1}) (*26*) that can be calculated as 34% and 84% for 1 and 10 mM bicarbonate, respectively.

Acetate Formation. To determine acetate formation, the reaction mixtures of pyruvate with peroxynitrite after 5 min incubation were analyzed by anion exchange chromatography as described in the Experimental Procedures. Acetate was identified by its retention time (2.6 min under the conditions employed) and by spiking with authentic acetate (data not shown). Trace amounts of acetate were detected when peroxynitrite was first added to the buffer to decompose before the addition of pyruvate (Table 2). Acetate yields were quantitated and compared with those obtained in 30 min incubations of hydrogen peroxide with pyruvate (Table 2). Yields were not stoichiometric, and in the case of peroxynitrite they accounted for 25% and 18% of the initial peroxynitrite concentration at pH 7.4 and 5.5, respectively (Table 2). Since bicarbonate inhibited the oxidation of pyruvate by peroxynitrite (Figures 7, 8) the low yields of acetate

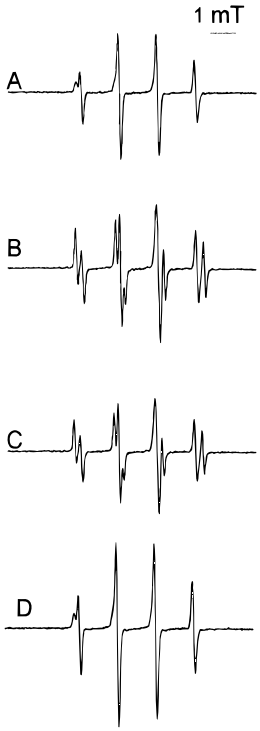

Figure 8. EPR spectra of DMPO radical adducts obtained during peroxynitrite decomposition in the presence of pyruvate and bicarbonate. The spectra were obtained after 1 min of incubation at room temperature of 0.5 mM peroxynitrite in 0.1 M phosphate buffer (pH 7.4) containing 0.1 mM DTPA with 0.1 M DMPO and (A) 0.5 mM GSH, (B) 0.5 mM GSH plus 50 mM pyruvate, (C) same as in B plus 1 mM bicarbonate, and (D) same as in B plus 10 mM bicarbonate. Instrumental conditions: microwave power, 20 mW; modulation amplitude, 0.1 mT; time constant, 0.2 s; scan rate, 0.05 mT/s; gain, 1.25×10^5.

Table 2. Production of Acetate during the Decarboxylation of Pyruvate Promoted by Peroxynitrite and Hydrogen Peroxide

system	acetate[a] (mM)
pyruvate (10 mM) + $ONOO^-$ (10 mM), pH 7.4	2.57 ± 0.23
$ONOO^-$ (10 mM) + pyruvate (10 mM), pH 7.4[b]	0.24 ± 0.07
pyruvate (10 mM) + $ONOO^-$ (10 mM), pH 5.5	1.81 ± 0.40
pyruvate (10 mM) + H_2O_2 (10 mM), pH 7.4	4.18

[a] Acetate was analyzed by anion exchange chromatography as described in the Experimental Procedures. The reaction mixtures in water, whose final pH was controlled by HCl and/or NaOH addition, were incubated for 5 and 30 min in the case of peroxynitrite and hydrogen peroxide, respectively. The values correspond to the mean ± SD of three independent experiments except for the hydrogen peroxide system whose value corresponds to the average of two experiments. [b] Peroxynitrite was added to the buffer to decompose before the addition of pyruvate (reverse addition experiment).

[3] Gatti, R. M., Alvarez, B., Vasquez-Vivar, J., Radi, R., and Augusto, O. Unpublished results.

Scheme 2

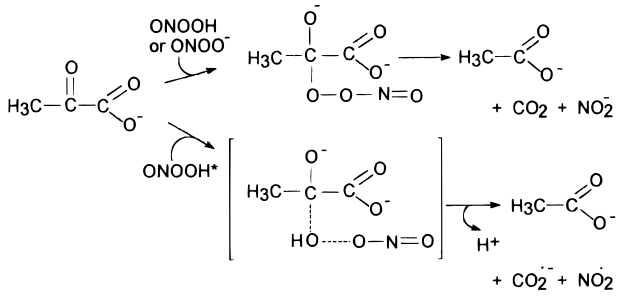

obtained (Table 2) may be due to the fast direct reaction between peroxynitrite and the produced carbon dioxide (*23*−*26*). A direct fast reaction between acetate and peroxynitrite was excluded by parallel stopped flow experiments (k < 5 M^{-1} s^{-1} at pH 7.4, 37 °C) (data not shown).

Discussion

Our results demonstrated that pyruvate reacts with peroxynitrite with an apparent second-order rate constant 1 order of magnitude higher than that of its reaction with hydrogen peroxide in phosphate buffer, pH 7.4, 37 °C (Figures 1−3). Both oxidants promoted decarboxylation of pyruvate to acetate (Table 2), but the process mediated by peroxynitrite also led to the formation of the carbon dioxide radical anion as attested by EPR spin-trapping (Figures 4, 6, 8) and oxygen consumption experiments (Figure 7; Table 1). Consequently, peroxynitrite-mediated decarboxylation of pyruvate provides yet another example of the ability of peroxynitrite to promote the one-electron oxidation of biomolecules in the absence of transition metal ions (*19*−*22*) by contrast with hydrogen peroxide-mediated one-electron oxidations (*43*). Accordingly, pyruvate decarboxylation by hydrogen peroxide produces the carbon dioxide radical anion only in the presence of iron(II)−EDTA (Figure 5).

It is difficult to estimate the fraction of peroxynitrite-mediated decarboxylation which proceeds through the one-electron oxidation pathway by spin-trapping experiments because the technique detects trapped rather than formed free radicals and radical adducts are not stable in the presence of peroxynitrite, requiring the presence of thiols to be detectable (*20, 28*). Thiols are oxidized to the corresponding thiyl radical by peroxynitrite (*20, 21, 28, 49, 50*), making it even more difficult to quantitate the formed free radical adducts. The suggestion that thiyl radicals are responsible for the generation of carbon dioxide radical anion in incubations of peroxynitrite, formate, and GSH (*49, 50*), however, should not apply to the oxidation of pyruvate since in this case the carbon dioxide radical anion cannot be formed by a simple hydrogen abstraction (see Scheme 2) as occurs during formate oxidation. In agreement, incubations of peroxynitrite with pyruvate consumed oxygen even in the absence of GSH (Figure 7). Consequently, oxygen consumption measurements should provide a better estimate of the formed carbon dioxide radical anion which reacts fast with oxygen (k = 2 × 10^9 M^{-1} s^{-1}) (*46*) in a 1:1 stoichiometry to form superoxide radical anion. Assuming such a stoichiometry, the fraction of peroxynitrite which produces carbon dioxide radical anion was estimated to be 4% and 2% at pH 5.1 and 7.5, respectively (Table 1). As pointed out in Results, however, secondary reactions of both carbon dioxide and carbon dioxide radical anion make it difficult to establish the total yield of the latter during the peroxynitrite-mediated decarboxylation of pyruvate. A role for hydrogen peroxide, eventually present as a contaminant in peroxynitrite stock solutions (*29, 30*), in mediating pyruvate decarboxylation was excluded by the slower rate of the hydrogen peroxide-promoted process (Figures 3, 5; Table 2). Oxidation of pyruvate by peroxynitrite produced acetate (Table 2) in much higher yields than free radicals estimated from oxygen uptake experiments (Table 1). About 20% and 2−4% of initial peroxynitrite concentrations produced acetate and free radicals, respectively. This comparison indicates that peroxynitrite-mediated pyruvate decarboxylation occurs through both one- and two-electron oxidation pathways, the latter being preponderant.

The reaction of pyruvate and other α-keto acids with hydrogen peroxide is proposed to occur through a two-electron pathway via the reversible formation of a tetrahedral intermediate and its subsequent irreversible decomposition to carbon dioxide, acetate, and water (*51, 52*) (Scheme 1). According to our results (Figure 5), only in the presence of transition metal ions is the tetrahedral intermediate reduced to the alkoxyl radical that generates carbon dioxide radical anion and acetate by β-scission (*53*) (Scheme 1).

A similar nucleophilic mechanism can account for the two-electron oxidative decarboxylation of pyruvate to carbon dioxide and acetate promoted by peroxynitrite (Scheme 2). The kinetic data obtained (Figures 1, 2) indicate that pyruvate can react with peroxynitrite anion (eq 8), peroxynitrous acid (eq 9), and activated peroxynitrous acid (eq 10). A direct reaction between pyruvate and the peroxynitrite anion is also supported by the inhibitory effects of the carbon dioxide/bicarbonate pair (Figures 7, 8) since the peroxynitrite-carbon dioxide adduct ($ONOOCO_2^-$) (*23*−*26*) is not expected to add to the carbonyl group of pyruvate (Scheme 2). The second-order rate constants of the reaction between pyruvate and peroxynitrite anion and peroxynitrous acid were estimated as 100 ± 7 and 49 ± 9 M^{-1} s^{-1}, respectively. Peroxynitrite anion is a better nucleophile than peroxynitrous acid, and this property appears to predominate over the charge repulsive effects involved in the reaction between the negatively charged pyruvate and peroxynitrite anion. It is possible that peroxynitrite anion attacks the enol form of pyruvate (CH_2=C−OH−CO_2^-) whose negative charge may be minimized by hydrogen bonding between the hydroxyl and carboxylate groups.[4] Most probably, peroxynitrite anion and peroxynitrous acid are responsible for the two-electron oxidation pathway producing carbon dioxide, whereas activated peroxynitrous acid should be responsible for the one-electron-mediated pathway (*19*−*22*) (Scheme 2). The latter species has been proposed to be a "tight" transition state with a lengthened O−O bond (16) which should favor the homolytic cleavage of the corresponding putative tetrahedral intermediate formed upon pyruvate attack leading to the formation of carbon dioxide radical anion.

The oxidation of α-keto acids, which are important cellular metabolites, by peroxynitrite may have several biological implications. The apparent second-order rate constant of the reaction of peroxynitrite with pyruvate

[4] We would like to thank one of the reviewers of our paper for bringing to our attention the possibility of peroxynitrite anion attacking the enol form of pyruvate.

at pH 7.4 (88 M^{-1} s^{-1}) is smaller than that determined for the reaction of the oxidant with other intracellular metabolites such as GSH (1350 M^{-1} s^{-1}, 37 °C) (*16*), but it is higher than the apparent second-order rate constant of the reaction between pyruvate and hydrogen peroxide (2.2 M^{-1} s^{-1}). Intracellular concentrations of pyruvate are on the order of 0.5 mM (*54*), and levels of 1.5 mM can be achieved in mitochondria (*55*). Consequently, pyruvate may act as a secondary defense line against both hydrogen peroxide- and peroxynitrite-mediated oxidations in special cellular environments such as mitochondria. Oxidation of α-keto acids by peroxynitrite, however, also leads to the formation of the carbon dioxide radical anion, although to a minor extent. The latter species can either produce superoxide anion and hydrogen peroxide under high oxygen tensions or reduce transition metal ions under reduced oxygen tensions, and all of these species can propagate free radical chain reactions. Depending on the biological environment, α-keto acids can either inhibit or propagate peroxynitrite-mediated oxidations. Under any circumstance, the reaction between pyruvate and peroxynitrite should be taken into account in unraveling the mechanisms by which pyruvate can induce a myriad of physiological responses (*1*−*8*).

Acknowledgment. We thank Dr. Lilian R. F. de Carvalho for providing access to the chromatograph and Dr. Beatriz Alvarez for helpful discussions. This work was supported by grants from the Fundação de Amparo à Pesquisa do Estado de São Paulo (FAPESP), Conselho Nacional de Desenvolvimento Científico e Tecnológico (CNPq), and Financiadora de Estudos e Projetos (FINEP) to O. Augusto, SAREC (Sweden) and CONICYT No. 138 (Uruguay) to R. Radi, and CONICYT No. 313 (Uruguay) to A. Denicola.

References

(1) Stanko, R. T., Mitrakou, A., Greenwalt, K., and Gerich, J. (1990) The effect of dihydroxyacetone and pyruvate on plasma glucose concentration and turnover in noninsulin-dependent diabetes mellitus. *Clin. Physiol. Biochem.* **8**, 283−288.

(2) Stanko, R. T., Mullick, P., Clarke, M. R., Contis, L. C., Janosky, J. E., and Ramasastry, S. S. (1994) Pyruvate inhibits grow of mammary carcinoma 13762 in rats. *Cancer Res.* **54**, 1004−1007.

(3) Nath, K. A., Ngo, E. O., Hebbel, R. P., Croatt, A. J., Zhou, B., and Nutter, L. M. (1995) α-Ketoacids scavenge H_2O_2 in vitro and in vivo and reduce menadione-induced DNA injury and cytotoxicity. *Am. J. Physiol.* **268**, C227−C236.

(4) Varma, S. D., and Devamanoharan, P. S. (1995) Oxidative denaturation of lens protein: prevention by pyruvate. *Ophthal. Res.* **27**, 18−22.

(5) Yanagida, S., Luo, C. S., Doyle, M., Pohost, G. M., and Pike, M. M. (1995) Nuclear magnetic resonance studies of cationic and energetic alterations with oxidant stress in perfused heart. Modulation with pyruvate and lactate. *Circ. Res.* **77**, 773−783.

(6) de Groot, M. J. M., van Helden, M. A. B., de Jong, Y. F., Coumans, W. A., and van der Vusse, G. J. (1995) The influence of lactate, pyruvate and glucose as exogenous substrates on free radical defense mechanisms in isolated rat hearts during ischaemia and reperfusion. *Mol. Cell. Biochem.* **146**, 147−155.

(7) O'Donnell-Tormey, J., Nathan, C. F., Lanks, K., DeBoer, C. J., and Harpe, J. (1987) Secretion of pyruvate. An antioxidant defense of mammalian cells. *J. Exp. Med.* **165**, 500−514.

(8) Stanko, R. T., Sekas, G., Isaacson, I. A., Clarke, M. R., Billiar, T. R., and Paul, H. S. (1995) Pyruvate inhibits clofibrate-induced hepatic peroxisomal proliferation and free radical production in rats. *Metabolism* **44**, 166−171.

(9) Holleman, M. A. F. (1904) Notice sur l'action de léau oxigénée sur les acides acétoniques et sur les dicétones 1.2. *Recl. Trav. Chim. Pays-Bas Belg.* **23**, 169−171.

(10) Huie, R. E., and Padmaja, S. (1993) The reaction of NO with superoxide. *Free Radical Res. Commun.* **18**, 195−199.

(11) Goldstein, S., and Czapski, G. (1995) The reaction of NO• with $O_2^{\bullet-}$ and $HO_2^{\bullet}$: A pulse radiolysis study. *Free Radical Biol. Med.* **19**, 505−510.

(12) Beckman, J. S., Beckman, T. W., Chen, J., Marshall, P. M., and Freeman, B. A. (1990) Apparent hydroxyl radical production by peroxynitrite: implications for endothelial injury from nitric oxide and superoxide. *Proc. Natl. Acad. Sci. U.S.A.* **87**, 1620−1624.

(13) Beckman, J. S., Ye, Y. Z., Anderson, P., Chen, J., Accavitti, M. A., Tarpey, M. M., and White, C. R. (1994) Extensive nitration of protein tyrosines in human atherosclerosis detected by immunohistochemistry. *Biol. Chem. Hoppe-Seyler* **375**, 81−88.

(14) Kooy, N. W., Royall, J. A., Ye, Y. Z., Kelly, D. R., and Beckman, J. S. (1995) Evidence for in vivo peroxynitrite production in human acute lung injury. *Am. J. Resp. Crit. Care Med.* **151**, 1250−1254.

(15) Giorgio, S., Linares, E., Capurro, M. de L., de Bianchi, A. G., and Augusto, O. (1996) Formation of nitrosyl hemoglobin and nitrotyrosine during murine leishmaniasis. *Photochem. Photobiol.* **63**, 750−754.

(16) Koppenol, W. H., Moreno, J. J., Pryor, W. A., Ischiropoulos, H., and Beckman, J. S. (1992) Peroxynitrite, a cloaked oxidant formed by nitric oxide and superoxide. *Chem. Res. Toxicol.* **5**, 834−841.

(17) Pryor, W. A., and Squadrito, G. L. (1995) The chemistry of peroxynitrite: a product from the reaction of nitric oxide with superoxide. *Am. J. Physiol. (Lung Cell Mol. Physiol.)* **268**, 699−722.

(18) Goldstein, S., Squadrito, G. L., Pryor, W. A., and Czapski, G. (1996) Direct and indirect oxidations by peroxynitrite, neither involving the hydroxyl radical. *Free Radical Biol. Med.* **21**, 965−974.

(19) Pryor, W. A., Jin, X., and Squadrito, G. L. (1994) One- and two-electron oxidations of methionine by peroxynitrite. *Proc. Natl. Acad. Sci. U.S.A.* **91**, 11173−11177.

(20) Augusto, O., Gatti, R. M., and Radi, R. (1994) Spin-trapping studies of peroxynitrite decomposition and of 3-morpholinosydnonimine N-ethylcarbamide autoxidation: direct evidence for metal-independent formation of free radical intermediates. *Arch. Biochem. Biophys.* **310**, 118−125.

(21) Vásquez-Vivar, J., Santos, A. M., Junqueira, V. B. C., and Augusto, O. (1996) Peroxynitrite-mediated formation of free radicals in human plasma: EPR detection of ascorbyl, albuminthiyl and uric acid-derived free radicals. *Biochem. J.* **314,** 869−876.

(22) Quijano, C., Alvarez, B., Gatti, R. M., Augusto, O., and Radi, R. (1997) Pathways of peroxynitrite oxidation of thiol groups. *Biochem. J.* **322**, 167−173.

(23) Lymar, S. V., and Hurst, J. K. (1995) Rapid reaction between peroxynitrite ion and carbon dioxide: implications for biological activity. *J. Am. Chem. Soc.* **117**, 8867−8868.

(24) Uppu, R. M., Squadrito, G. L., and Pryor, W. A. (1996) Acceleration of peroxynitrite oxidations by carbon dioxide. *Arch. Biochem. Biophys.* **372**, 335−343.

(25) Lymar, S. V., Jiang, Q., and Hurst, J. K. (1996) Mechanism of carbon dioxide-catalyzed oxidation of tyrosine by peroxynitrite. *Biochemistry* **35**, 7855−7861.

(26) Denicola, A., Freeman, B. A., Trujillo, M., and Radi, R. (1996) Peroxynitrite reaction with carbon dioxide/bicarbonate: kinetics and influence on peroxynitrite-mediated oxidations. *Arch. Biochem. Biophys.* **333**, 49−58.

(27) Edwards, J. O., and Plumb, R. C. (1994) The chemistry of peroxonitrites. *Prog. Inorg. Chem.* **41**, 599−635.

(28) Augusto, O., Radi, R., Gatti, R. M., and Vásquez-Vivar, J. (1996) Detection of secondary radicals from peroxynitrite-mediated oxidations by electron spin resonance. *Methods Enzymol.* **269** (Part B), 346−354.

(29) Beckman, J. S., Chen, J., Ischiropoulos, H., and Crow, J. P. (1994) Oxidative chemistry of peroxynitrite. *Methods Enzymol.* **233**, 229−250.

(30) Pryor, W. A., Cueto, R., Jin, X., Koppenol, W. H., Ngu-Schwemlein, M., Squadrito, G. L., Uppu, P. L., and Uppu, R. M. (1995) A practical method for preparing peroxynitrite solutions of low ionic strength and free of hydrogen peroxide. *Free Radical Biol. Med.* **18**, 75−83.

(31) Radi, R., Turrens, J. F., Chang, L. Y., Bush, K. M., Crapo, J. D., and Freeman, B. A. (1991) Detection of catalase in rat heart mitochondria. *J. Biol. Chem.* **266**, 22028−22034.

(32) Robinson, J., and Cooper, J. M. (1970) Method of determining oxygen concentration in biological media, suitable for calibrations of the oxygen electrode. *Anal. Biochem.* **33**, 390−399.

(33) Alvarez, B., Denicola, A., and Radi, R. (1995) Reaction between peroxynitrite and hydrogen peroxide: formation of oxygen and slowing of peroxynitrite decomposition. *Chem. Res. Toxicol.* **8**, 859−864.

(34) Squadrito, G. L., Jin, X., and Pryor, W. A. (1995) Stopped-flow kinetic study of the reaction of ascorbic acid with peroxynitrite. *Arch. Biochem. Biophys.* **322**, 53−59.

(35) Alvarez, B., Rubbo, H., Kirk, M., Barnes, S., Freeman, B. A., and Radi, R. (1996) Peroxynitrite dependent tryptophan nitration. *Chem. Res. Toxicol.* **9**, 390−396.
(36) Darley, K. S. (1978) Ph.D. Dissertation, University of Toronto; *Dis. Abstr. Int.* **B93**, 3428 (1979).
(37) Lemercier, J. N., Squadrito, G. L., and Pryor, W. A. (1995) Spin-trap studies on the decomposition of peroxynitrite. *Arch. Biochem. Biophys.* **321**, 31−39.
(38) Pou, S., Nguyen, S. Y., Gladwell, T., and Rosen, G. M. (1995) Does peroxynitrite generate hydroxyl radical? *Biochim. Biophys. Acta* **1244**, 62−68.
(39) Popp, J. L., Kalyanaraman, B., and Kirk, T. K. (1990) Lignin peroxidase oxidation of Mn^{2+} in the presence of veratryl alcohol, malonic or oxalic acid, and oxygen. *Biochemistry* **29**, 10475−10480.
(40) Connor, H. D., Thurman, R. D., Galizi, M. D., and Mason, R. P. (1986) The formation of a novel free radical metabolite from CCl_4 in the perfused rat liver in vivo. *J. Biol. Chem.* **261**, 4542−4548.
(41) Kalyanaraman, B., Janzen, E. G., and Mason, R. P. (1985) Spin trapping of the azidyl radical in azide/catalase/H_2O_2 and various azide/peroxidase/H_2O_2 peroxidizing systems. *J. Biol. Chem.* **260**, 4003−4006.
(42) Buettner, G. R., and Mason, R. P. (1990) Spin-trapping methods for detecting superoxide and hydroxyl free radicals in vitro and in vivo. *Methods Enzymol.* **186**, 127−133.
(43) Koppenol, W. H. (1994) Chemistry of iron and copper in radical reactions. In *Free Radical Damage and Its Control* (Rice-Evans, C. A., and Burdon, R. H., Eds.) pp 3−24, Elsevier Science B.V., London.
(44) Finkelstein, E., Rosen, G. M., and Rauckman, E. J. (1980) Spin trapping. Kinetics of the reaction of superoxide and hydroxyl radicals with nitrones. *J. Am. Chem. Soc.* **102**, 4994−4999.
(45) Kraljic, I. (1967) Kinetics of OH radical reactions in radiolysis, photolysis and the Fenton system. In *The Chemistry of Ionization and Excitation* (Johnson, G. R. A., and Scholes, G., Eds.) pp 302−309, Taylor B. Francis Ltd., London.
(46) Adams, G. E., and Wilson, R. L. (1969) Pulse radiolysis studies on the oxidation of organic radicals in aqueous solution. *Trans. Faraday Soc.* **65**, 2981−2987.
(47) Radi, R., Beckman, J. S., Bush, K. M., and Freeman, B. A. (1991) Peroxynitrite-induced membrane lipid peroxidation: cytotoxic potential of superoxide and nitric oxide. *Arch. Biochem. Biophys.* **288**, 481−487.
(48) Steenken, S., Sprague, E. D., and Schulte-Frohlinde, D. (1975) Photofragmentation of α-oxocarboxylic acids in aqueous solution. An EPR study. Formation of semidione radicals by decarboxylative substitution of α-oxocarboxylic acids by acyl radicals-I: glyoxilic, pyruvic, α-oxocarbutyric, α-oxoglutaric and α-oxoisocaproic acids. *Photochem. Photobiol.* **22**, 19−27.
(49) Karoui, H., Hogg, N., Fréjaville, C., Tordo, P., and Kalyanaraman, B. (1996) Characterization of sulfur centered radical intermediates formed during the oxidation of thiols and sulfite by peroxynitrite. *J. Biol. Chem.* **271**, 6000−6009.
(50) Karoui, H., Hogg, N., Joseph, J., and Kalyanaraman, B. (1996) Effect of superoxide dismutase mimics on radical adduct formation during the reaction between peroxynitrite and thiols-An ESR-spin trapping study. *Arch. Biochem. Biophys.* **330**, 115−124.
(51) Melzer, E., and Schmidt, H. L. (1988) Carbon isotope effects on the decarboxylation of carboxylic acids. Comparison of the lactate oxidase reaction and the degradation of pyruvate by H_2O_2. *Biochem. J.* **252**, 913−915.
(52) Siegel, B., and Lanphear, J. (1979) Kinetics and mechanisms for the acid-catalyzed oxidative decarboxylation of benzoylformic acid. *J. Org. Chem.* **44**, 942−946.
(53) Bernardi, R., Caronna, T., Galli, R., Minisci, F., and Perchinunno, M. (1973) Nucleophilic character of carbon free radicals a new convenient, selective carbozylation of heteroaromatic bases. *Tetrahedron Lett.* **9**, 645−648.
(54) Hems, D. A., and Brosnan, J. T. (1970) Effect of ischaemia on content of metabolites in rat liver and kidney in vivo. *Biochem. J.* **120**, 105−111.
(55) Aw, T. Y., Andersson, B. S., and Jones, D. P. (1987) Mitochondrial transmembrane ion distribution during anoxia. *Am. J. Physiol.* **252** (Cell Physiol. 21), C356−C361.

TX970031G